

Article

Population Genetic Structure and Diversity of *Metaphire remanens* (Oligochaeta: Megascolecidae) Based on Mitochondrial DNA Analysis, with a Note on a New Species of *Metaphire remanens* sp. nov.

Qing Jin ^{1,2}, Jibao Jiang ^{1,2,*}, Jiali Li ^{1,2} and Jiangping Qiu ^{1,2,*}

¹ School of Agriculture and Biology, Shanghai Jiao Tong University, Shanghai 200240, China; jq20190001@sjtu.edu.cn (Q.J.); 18786636984@sjtu.edu.cn (J.L.)

² Shanghai Urban Forest Research Station, State Forestry Administration, Shanghai 200240, China

* Correspondence: jjb12342004@gmail.com (J.J.); jpq@sjtu.edu.cn (J.Q.)

Abstract: *Metaphire remanens* sp. nov. is widely distributed throughout Hunan Province, China. We sequenced the mitochondrial DNA to investigate its population genetic structure and genetic diversity, including cytochrome c oxidase subunit I, cytochrome c oxidase subunit II, 12S ribosomal (r)RNA, 16S rRNA, and nicotinamide adenine dinucleotide dehydrogenase subunit 1, derived from 39 individuals from seven geographic locations in Hunan Province. The genetic diversity indices showed that populations of *M. remanens* have a strong genetic structure and obvious dispersal histories. *M. remanens* did not experience population expansion, except in Xiangtan City. This may be because of its evolution toward parthenogenesis. The divergence time estimates indicated that *M. remanens* originated at 19.2055 Ma and then generated two main lineages at 1.7334 Ma (Quaternary glaciation). These results indicate that glaciation, geographic isolation, and dispersal ability are significant factors that influence the differentiation and dispersal of *M. remanens*. In this study, we describe *Metaphire remanens* sp. nov. in morphology.

Keywords: earthworm; *Metaphire remanens* sp. nov.; mitochondrial gene; population genetic structure; genetic diversity



Citation: Jin, Q.; Jiang, J.; Li, J.; Qiu, J. Population Genetic Structure and Diversity of *Metaphire remanens* (Oligochaeta: Megascolecidae) Based on Mitochondrial DNA Analysis, with a Note on a New Species of *Metaphire remanens* sp. nov. *Diversity* **2022**, *14*, 275. <https://doi.org/10.3390/d14040275>

Academic Editors: Michael Wink and Daniel Fernández Marchán

Received: 16 February 2022

Accepted: 3 April 2022

Published: 6 April 2022

Publisher's Note: MDPI stays neutral with regard to jurisdictional claims in published maps and institutional affiliations.



Copyright: © 2022 by the authors. Licensee MDPI, Basel, Switzerland. This article is an open access article distributed under the terms and conditions of the Creative Commons Attribution (CC BY) license (<https://creativecommons.org/licenses/by/4.0/>).

1. Introduction

Earthworms (order Oligochaeta) are among the most important soil fauna and play an important role in soil structure, ecology, and biogeochemical cycles [1,2]. Moreover, earthworms are one of the few hermaphroditic groups in the animal kingdom [3–5]. In theory, parthenogenetic species have fewer evolutionary advantages than species engaging in bisexual reproduction do, but many parthenogenetic species can successfully occupy certain distribution areas for survival. Their genetic diversity evolves at a measurable rate and is not significantly reduced [6,7]. In addition, some parthenogenetic species multiply more rapidly than sexual species; thus, this reproductive mode has gained attention in both biodiversity research and agricultural production [8,9].

Metaphire remanens sp. nov. has a tendency toward parthenogenesis, displaying a lack of male pores, degeneration of prostate glands, and loss of seminal vesicles [10]. *M. remanens* is widely distributed in Hunan Province; however, its differentiation and spread remain unclear. Parthenogenesis, geological events, climate change, and human activity are key factors that play important roles in the differentiation and dispersal of earthworms [11–15]. Mitochondrial genes cytochrome c oxidase subunit I (COI), cytochrome c oxidase subunit II (COII), 12S ribosomal (r)RNA (12S), 16S rRNA (16S), and nicotinamide adenine dinucleotide dehydrogenase subunit 1 (ND1) are effective tools for studying the molecular phylogeny and phylogeography of earthworms [11,16,17]. They provide an accurate technical means for defining the genera and species of earthworms and determining

phylogenetic relationships among species. They also provide the possibility of exploring the origin, differentiation, and dispersal of earthworms at the molecular level.

In this study, 39 samples, from seven cities in Hunan Province, were collected to cluster mitochondrial genes, and the following results were obtained: (1) population genetic diversity of *Metaphire remanens*; (2) population differentiation and dispersal of *M. remanens*; and (3) divergence times and histories of *M. remanens*. The aim of this study was to reveal the possible population genetic structure of *M. remanens* and explore its possible formation mechanism.

2. Materials and Methods

2.1. Earthworm Sampling

A total of 123 *Metaphire remanens* individuals were collected from seven cities in Hunan Province, China, in 2019 (Figure 1, Table 1). One individual, *Amyntas pectiniferus* (Michaelsen, 1931), was collected as an outgroup in Shanghai City, China (F03: SH201001-03, 121.459° E, 31.029° N). First, the collected individuals were washed with clean water. Then, they were anaesthetized in a 10% ethanol solution, fixed in anhydrous alcohol, and preserved in a 95% ethanol solution. Morphological characteristics of the individuals were identified using a stereomicroscope. The tail muscle tissue (approximately 0.02 g) was removed and cleaned for DNA extraction.

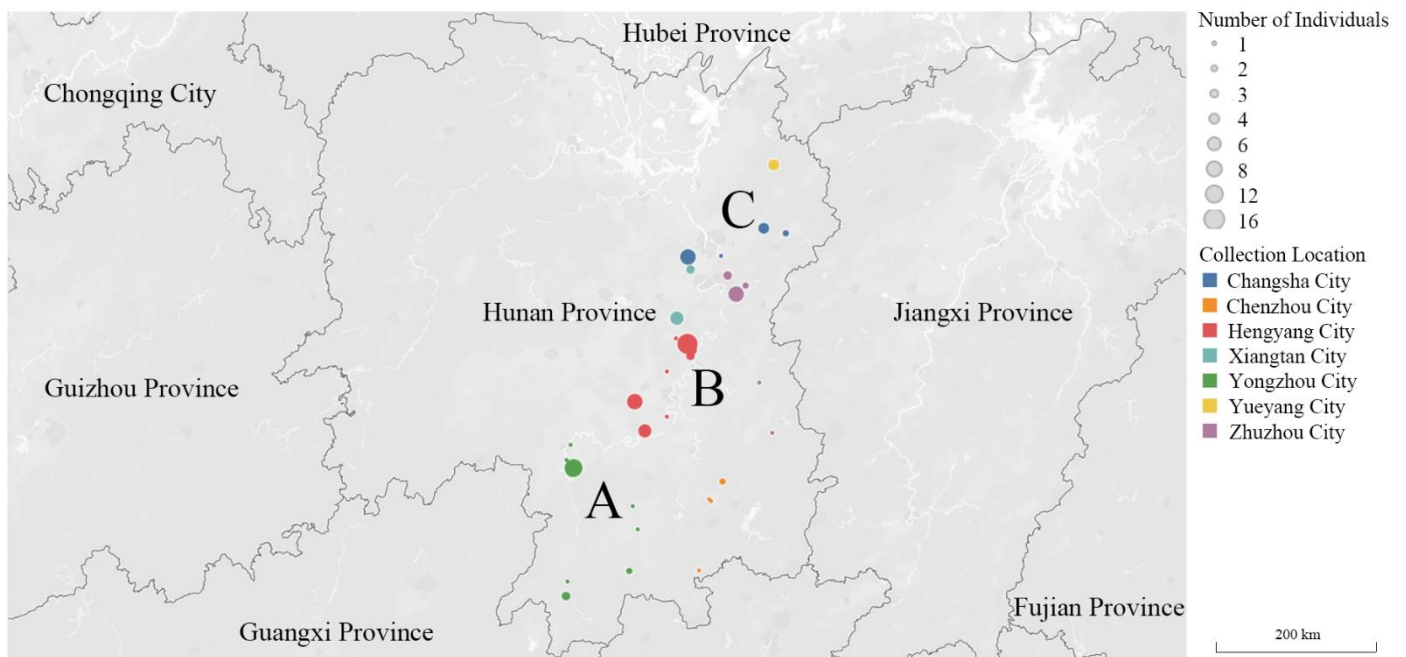


Figure 1. Sampling locations (39) in Hunan Province. Region A represent the southern part of Hunan Province (Yongzhou and Chenzhou City); Region B represents the central part of Hunan Province (Hengyang, Zhuzhou, and Xiangtan City); Region C represents the northern part of Hunan Province (Changsha and Yueyang City); Region D (not shown) represents Shanghai City.

2.2. DNA Extraction, Amplification, and Sequencing

Total genomic DNA was extracted using the E.Z.N.A.[®] Mollusc DNA kit (Omega Bio-Tek, Norcross, GA, USA), according to the manufacturer's instructions. We examined the quality of the DNA samples by electrophoresis on 1% agarose gel. They were then stored at -20°C .

We amplified mitochondrial genes using a 50 μL reaction mixture with 35.4 μL double-distilled H_2O , as well as 9.6 μL Trans Taq[™] polymerase high fidelity containing 0.6 μL TransTaq[™] HiFi DNA polymerase, 4 μL 2.5 mM dNTPs, 5 μL 10 \times TransTaq[™] HiFi Buffer I, 1 μL DNA template, and 2 μL of each primer. The polymerase chain reaction (PCR) of COI, COII, 12S, 16S, and ND1 was carried out as follows: 5 min at 94°C , followed by

32 cycles at 94 °C for 30 s, 50 °C for 30 s, and 72 °C for 60 s, with a final 10 min extension at 72 °C [18,19].

The Beijing Genomics Institute (Shanghai, China) visualized the PCR products on a 1% agarose gel, purified them, and sequenced them [20,21].

Table 1. Collection information on *M. remanens* sequenced in this study.

Label	Collection Location	Longitude (°E)	Latitude (°N)	Collection Date	Elevation (m)	Gene Code	Number
P1CJHUSH190510089N5-01	Changsha City	112.784	28.086	10 May 2019	47	Y1014	8
P1CJHUSH190510089N5-02	Changsha City	112.784	28.086	10 May 2019	47	Y1015	1
P1CJHUSH190528089N9-04	Changsha City	113.102	28.094	28 May 2019	24	Y1033	1
P1CJHUSH190510779N4-04	Changsha City	113.726	28.2831	10 May 2019	70.65	Y1664	2
P1CJHUSH190511779N9-01	Changsha City	113.52	28.3279	11 May 2019	112.45	Y1676	4
P1CJHUSH190511779N9-02	Changsha City	113.52	28.3279	11 May 2019	112.45	Y1677	1
P1CJHUSH190510083N1-04	Xiangtan City	112.816	27.983	10 May 2019	47	Y1039	1
P1CJHUSH190510083N1-08	Xiangtan City	112.816	27.983	10 May 2019	47	Y1043	3
P1CJHUSH190511083Q8-04	Xiangtan City	112.681	27.568	11 May 2019	88	083Q804	6
P1CJHUSH190512778Q9-03	Yueyang City	113.6092	28.8567	12 May 2019	178.15	Y1702	4
P1CJHUSH190512784N3-03	Hengyang City	112.815	27.246	12 May 2019	96	784N303	3
P1CJHUSH190512784N4-04	Hengyang City	112.818	27.299	12 May 2019	67	Y1078	1
P1CJHUSH190512784N4-05	Hengyang City	112.818	27.299	12 May 2019	67	Y1079	4
P1CJHUSH190512784N5-01	Hengyang City	112.78	27.346	12 May 2019	114	Y1080	16
P1CJHUSH190512784R7-05	Hengyang City	112.669	27.395	12 May 2019	88	Y1085	1
P1CJHUSH190512079N3-01	Hengyang City	112.583	27.113	12 May 2019	110	Y1105	1
P1CJHUSH190513074N1-05	Hengyang City	112.585	26.721	13 May 2019	60	Y1122	1
P1CJHUSH190513074Q5-03	Hengyang City	112.372	26.601	13 May 2019	88	Y1128	6
P1CJHUSH190513074Q5-05	Hengyang City	112.372	26.601	13 May 2019	88	Y1129	1
P1CJHUSH190513074R8-01	Hengyang City	112.272	26.852	13 May 2019	106	074R801	8
P1CJHUSH190515072N4-04	Yongzhou City	111.661	26.483	16 May 2019	107	Y1184	1
P1CJHUSH190516072Q6-01	Yongzhou City	111.625	26.353	16 May 2019	116	Y1187	1
P1CJHUSH190516072Q8-01	Yongzhou City	111.691	26.283	16 May 2019	129	Y1189	12
P1CJHUSH190516072N9-03	Yongzhou City	111.674	26.252	16 May 2019	117	072N903	4
P1CJHUSH190517069N4-01	Yongzhou City	111.617	25.173	17 May 2019	219	Y1226	3
P1CJHUSH190517069N8-03	Yongzhou City	111.634	25.301	17 May 2019	201	069N803	1
P1CJHUSH190518807N4-02	Yongzhou City	112.227	25.398	18 May 2019	258	Y1253	2
P1CJHUSH190519808R2-02	Yongzhou City	112.31	25.753	19 May 2019	204	Y1285	1
P1CJHUSH190519808Q7-05	Yongzhou City	112.258	25.951	19 May 2019	230	Y1304	1
P1CJHUSH190520798N9-03	Chenzhou City	113.008	25.997	20 May 2019	90	Y1332	1
P1CJHUSH190520798Q10-01	Chenzhou City	112.988	26.015	20 May 2019	106	Y1334	1
P1CJHUSH190521799N1-03	Chenzhou City	112.897	25.4	21 May 2019	259	Y1363	1
P1CJHUSH190521800N5-04	Chenzhou City	113.125	26.167	21 May 2019	92	Y1347	2
P1CJHUSH190524073N1-03	Zhuzhou City	113.598	26.585	24 May 2019	174	Y1508	1
P1CJHUSH190525780Q2-01	Zhuzhou City	113.47	27.013	25 May 2019	151	Y1539	1
P1CJHUSH190527082Q1-01	Zhuzhou City	113.347	27.842	27 May 2019	82	Y1614	2
P1CJHUSH190527082N5-01	Zhuzhou City	113.251	27.771	27 May 2019	56	Y1634	4
P1CJHUSH190527082N5-02	Zhuzhou City	113.251	27.771	27 May 2019	56	Y1635	8
P1CJHUSH190528082N8-01	Zhuzhou City	113.164	27.93	28 May 2019	34	Y1645	3

2.3. Sequence Alignment, Population Genetic Structure and Diversity, Divergence Time, and Spread History

We evaluated population genetic structure and diversity, divergence time, and spread history using a combination of COI + COII + 12S + 16S + ND1 with one *Amyntas pectiniferus* as an outgroup. We aligned the sequences and combined the datasets using Geneious Prime 2022.

We estimated the corresponding parameters using jModelTest v.2.1.7 [22]. We selected the best-fitting models for the phylogenetic estimation of Bayesian phylogeny estimation (BI) analyses. jModeltest showed that GTR + I + G was the best-fitting model for the COI + COII + 12S + 16S + ND1 gene (3803 bp), with a gamma shape parameter of 0.1810.

Phylogenetic trees were reconstructed based on the COI + COII + 12S + 16S + ND1 gene datasets of 39 *M. remanens* individuals and one *A. pectiniferus* individual as the outgroup. BI was performed using MrBayes version 3.2.6 [23]. Posterior probabilities and bootstrap support of each branch were calculated from the sampled trees. Another phylogenetic tree of new species and some similar species was reconstructed by using a BI method, based on the COI gene datasets of *M. remanens*, *Metaphire acincta* (Goto and Hatai, 1899), *Metaphire californica* (Kinberg, 1867), *Metaphire communissima* (Goto and Hatai, 1898), *Metaphire guillelmi* (Michaelsen, 1895), *Metaphire yamadai* (Hatai, 1930), *Metaphire saxicalcis* Bantaowong 2016, *Metaphire vesiculate* (Goto and Hatai, 1899), *Metaphire vulgaris* (Chen,

1930), and *Metaphire peguana* (Rosa, 1890). jModeltest showed that GTR + I + G was the best-fitting model for the COI gene (616 bp), with a gamma shape parameter of 0.3540.

We evaluated population structure using Arlequin v.3.5.2 [24]. We then constructed a haplotype network to infer relationships among haplotypes, as well as their geographical distribution using PopART v.1.7 [25]. Nucleotide mismatch distribution analyses were performed using DnaSP 6.0 [26]. Neutrality tests were used to test population equilibrium.

We calculated the basic statistics of mitochondrial DNA diversity, including nucleotide and haplotype diversity, Tajima's D and Fu's F_s neutrality tests, and nucleotide mismatch distribution analysis between and within lineages, using DnaSP 6.0 [26–28]. We constructed a Bayesian skyline plot (BSP), with BEAST 1.8.2 and Tracer 1.7, to infer the timing of population events [29,30]. We reconstructed the ancestral distribution area using RASP v.3.2.

We estimated the Bayesian tree and divergence time of *M. remanens* using BEAST 1.8.2, based on 3803 bp segments, comprising of mitochondrial genes COI, COII, 12S, 16S, and ND1, with one *A. pectiniferus* as an outgroup [29]. Since earthworms lack a fossil record, the age of the calibration clade between *M. remanens* and *A. pectiniferus* was set at a mean age of 30.19 Ma (95% 25.74–34.89 Ma). The base substitution rate was set to 0.025 for COI and 0.012 for 12S, referring to previous research [10,31]. The result was obtained with 50,000,000 MCMC steps, and the first 20% served as burn-in. The output was visualized in Tracer 1.7 to determine whether all parameters achieved convergence and suitable effective sample sizes. All trees were visualized and edited using FigTree v2.1.4.

3. Results

3.1. Population Genetic Structure and Diversity

We compared the COI gene sequences of the 39 individuals, and the pairwise distance of COI was 0.0–6.6% (Table 2). We plotted the posterior probabilities of the Bayesian analysis on the BI tree (Figure 2). *M. remanens* consisted of five clades (Clades 1–5). Clade 1 was distributed mainly in Hengyang and Zhuzhou City; Clade 2 was distributed mainly in Hengyang and Yongzhou cities; Clade 3 was distributed mainly in Changsha, Yongzhou, and Chenzhou cities; Clade 4 was distributed in Hengyang City; and Clade 5 was distributed mainly in Changsha, Yongzhou, and Zhuzhou cities. Samples from the same or adjacent areas were clustered. According to the results of the pairwise distance of COI and the phylogenetic tree, Clade 5 may be a cryptic species.

We constructed a haplotype network, with a 617 bp fragment of COI, from 39 individuals, at seven locations (Figure 3). The haplotype network included ten haplotypes. Hap_2, Hap_5, and Hap_9 were shared haplotypes; Hap_1, Hap_3, Hap_4, and Hap_6–10 were unique haplotypes. Hap_5 was the most widely scattered haplotype, present in individuals from Changsha, Yueyang, Yongzhou, Chenzhou, and Zhuzhou cities. Individuals from Changsha and Hengyang cities contained the most unique haplotypes. The haplotype network exhibited a certain level of population genetic structure, which was in concordance with the phylogenetic trees. Clade 1 included Hap_1 and Hap_5; Clade 2 included Hap_1 and Hap_2; Clade 3 included Hap_1, Hap_3, and Hap_10; Clade 4 contained Hap_6–8; Clade 5 included Hap_4 and Hap_9.

All 39 individuals, from the seven locations, produced high-quality DNA and were successfully sequenced for the COI + COII + 12S + 16S + ND1 gene. The average base composition of the fragment revealed an intense bias of A + T (A, 36.3%; C, 19.4%; G, 15.2%; T, 29.1%), which is common in the mitochondrial genomes of invertebrates [32]. With the exception of the population from Xiangtan and Chenzhou City, populations from other cities contained many polymorphic sites and high nucleotide diversity (Table 3). All populations showed a high diversity. These results indicated that every population had exclusive haplotypes, suggesting that great genetic differentiation exists between lineages.

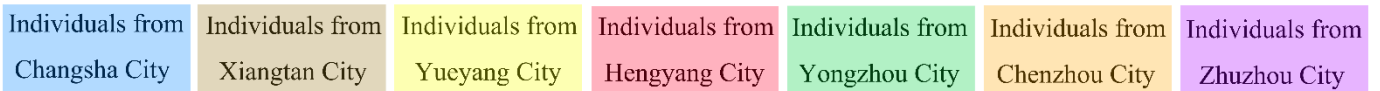
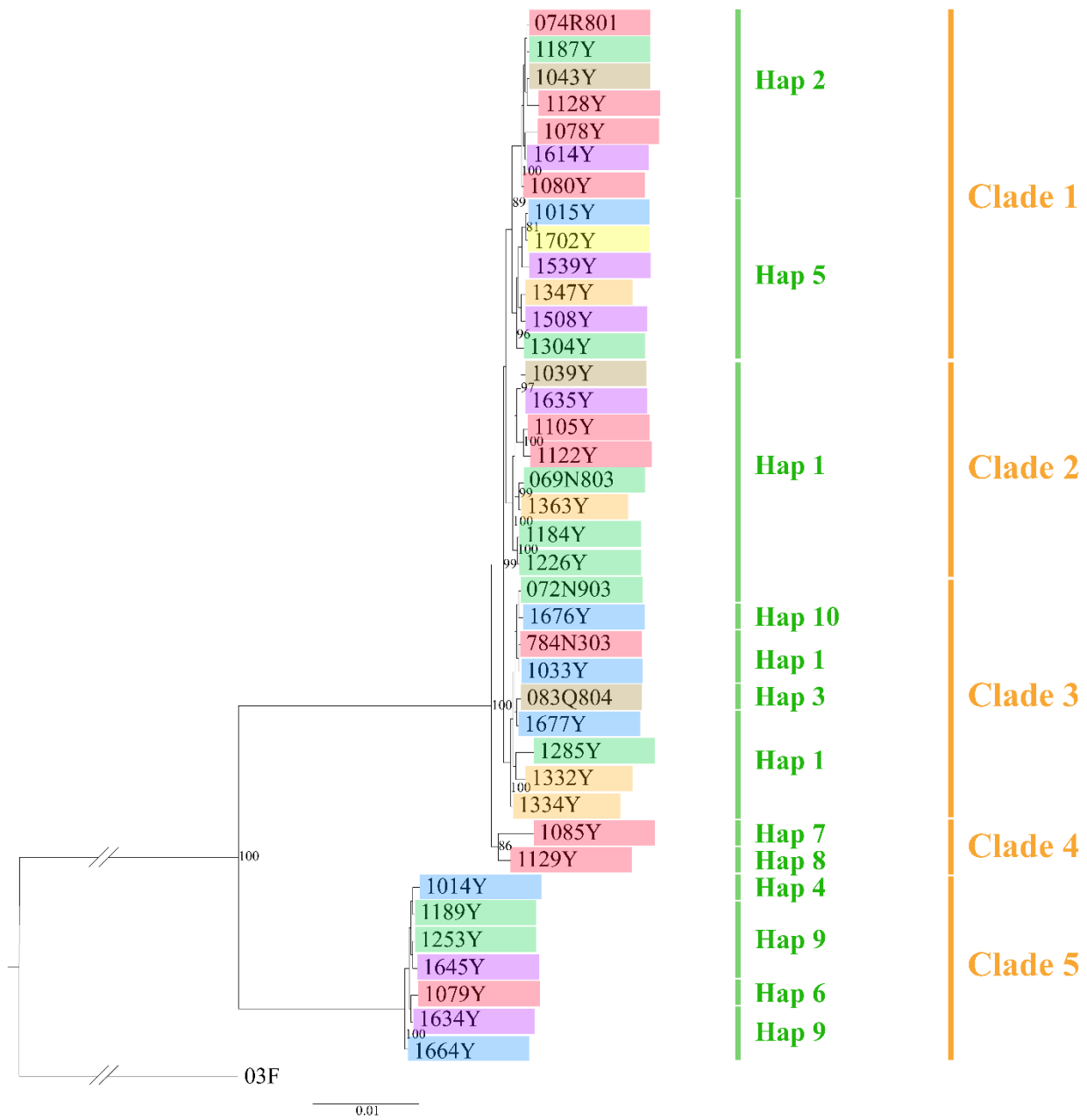


Figure 2. Phylogenetic trees, reconstructed using Bayesian phylogeny estimation, based on COI + COII + 12S + 16S + ND1 genes. Bayesian posterior probabilities ($pp \geq 0.95$) are shown on the branches. *Amynthes pectiniferus* (03F) was used as the outgroup taxon.

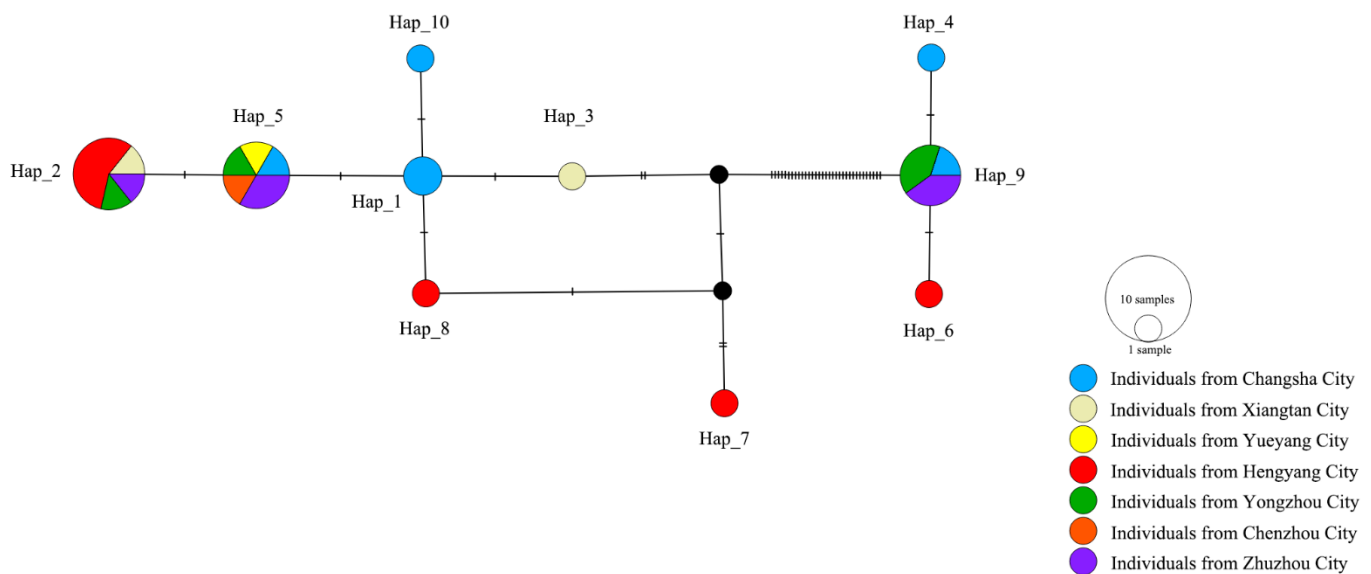


Figure 3. Unrooted network of 10 haplotypes in 39 individuals of *M. remanens* from 7 locations, based on 617 bp of COI gene. Each circle in the haplotype network is homologous with one haplotype, and its size is proportional to its frequency among samples. Dark dots represent intermediate haplotypes that were not sampled or died out.

Table 3. Summaries of genetic diversity measurement and neutrality tests, based on the COI + COII + 12S + 16S + ND1 gene.

Collection Location	Number of Sequences Used	Polymorphic Sites	Nucleotide Diversity	Number of Haplotypes	Haplotype Diversity	Fu's FS	Tajima's D
Changsha City	6	152	0.02183	5	0.933	4.460	1.30792, $p > 0.10$
Xiangtan City	3	11	0.00203	3	1.000	0.807	—
Yueyang City	1	—	—	—	—	—	—
Hengyang City	10	176	0.01090	9	0.978	1.042	$-1.85453, p < 0.05$
Yongzhou City	9	159	0.01714	7	0.944	4.360	0.17225, $p > 0.10$
Chenzhou City	4	10	0.00143	4	1.000	-0.480	$-0.52807, p > 0.10$
Zhuzhou City	6	150	0.02213	6	1.000	1.591	1.26797, $p > 0.10$
Hunan Province	39	176	0.01366	25	0.960	2.611	0.37830, $p > 0.10$

3.2. Divergence Time and Colonization History

The root of the tree, homologous to the speciation of *M. remanens* and *A. pectiniferus*, was estimated to have occurred at approximately 19.2055 Ma. The two main lineages of *M. remanens* formed (Clades 1–4 and 5) at approximately 1.7334 Ma (Figure 4).

Tajima's D values were not significant, except for the population from Xiangtan City (Table 3). The outcome of nucleotide mismatch distribution analysis, based on fragments of COI + COII + 12S + 16S + ND1, showed the following: multimodal distribution for six cities and Hunan Province and a transition for Xiangtan City (Figure 5). This result is consistent with Tajima's D values. The results revealed that *M. remanens* in Xiangtan City experienced population expansion. Bayesian skyline plots (BSP) showed an explicit demographic history of the populations of *M. remanens* (Figure 6). During the climatic fluctuations in the last glacial age (MIS 2–4), no change in the population history. Shortly, the population suddenly decreased during the last ice age.

A distribution map of the ancestral region indicated that *M. remanens* in Hunan Province originated in Region B (the central part of Hunan Province) (Figure 7). It then spreads from Region B to Region C (northern part of Hunan Province) and Region A (southern part of Hunan Province).

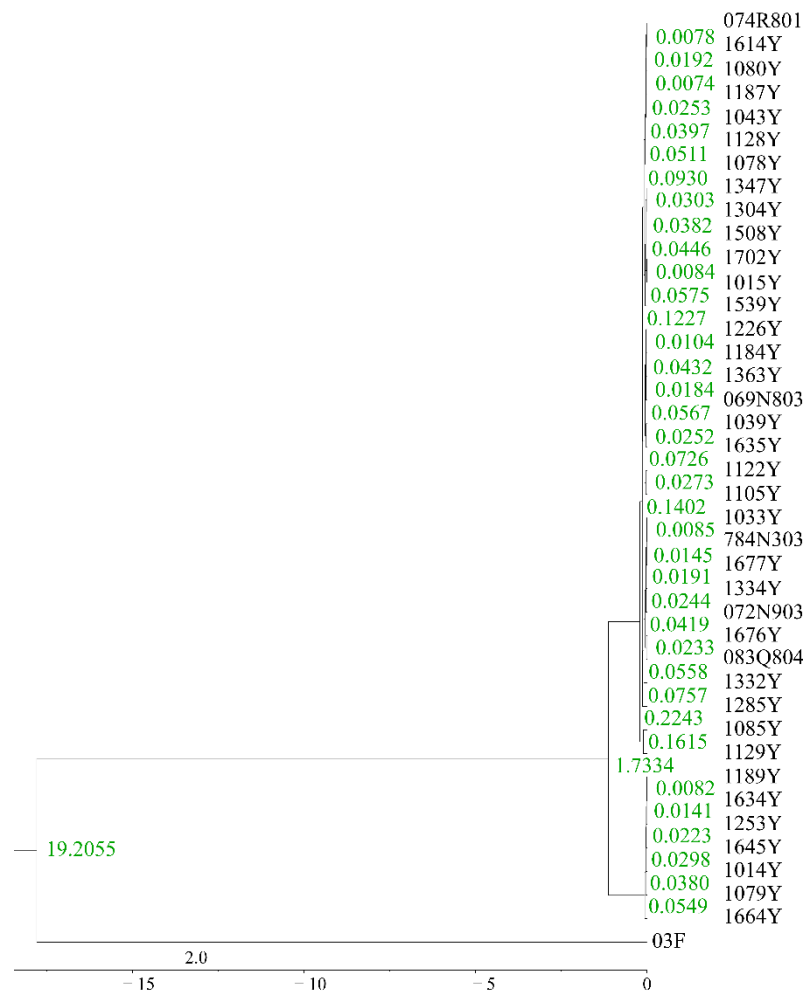


Figure 4. Divergence times estimated for *M. remanens* using COI + COII + 12S + 16S + ND1, based on a relaxed molecular clock.

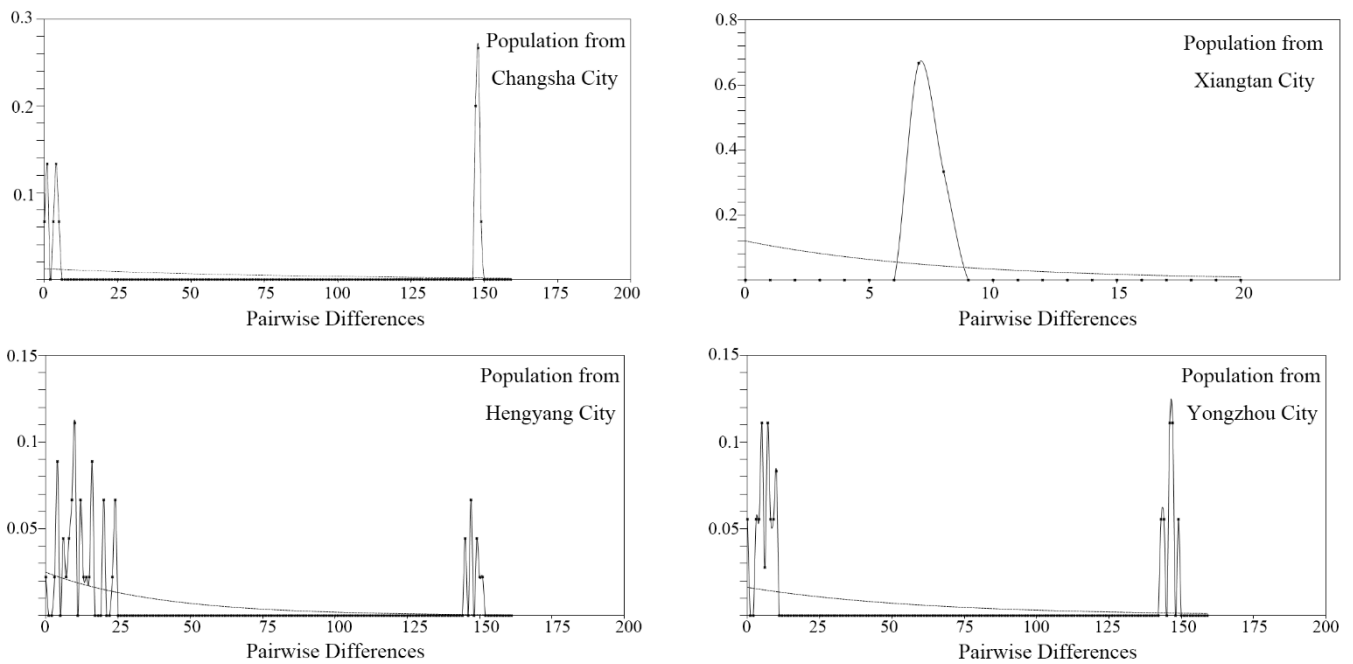


Figure 5. Cont.

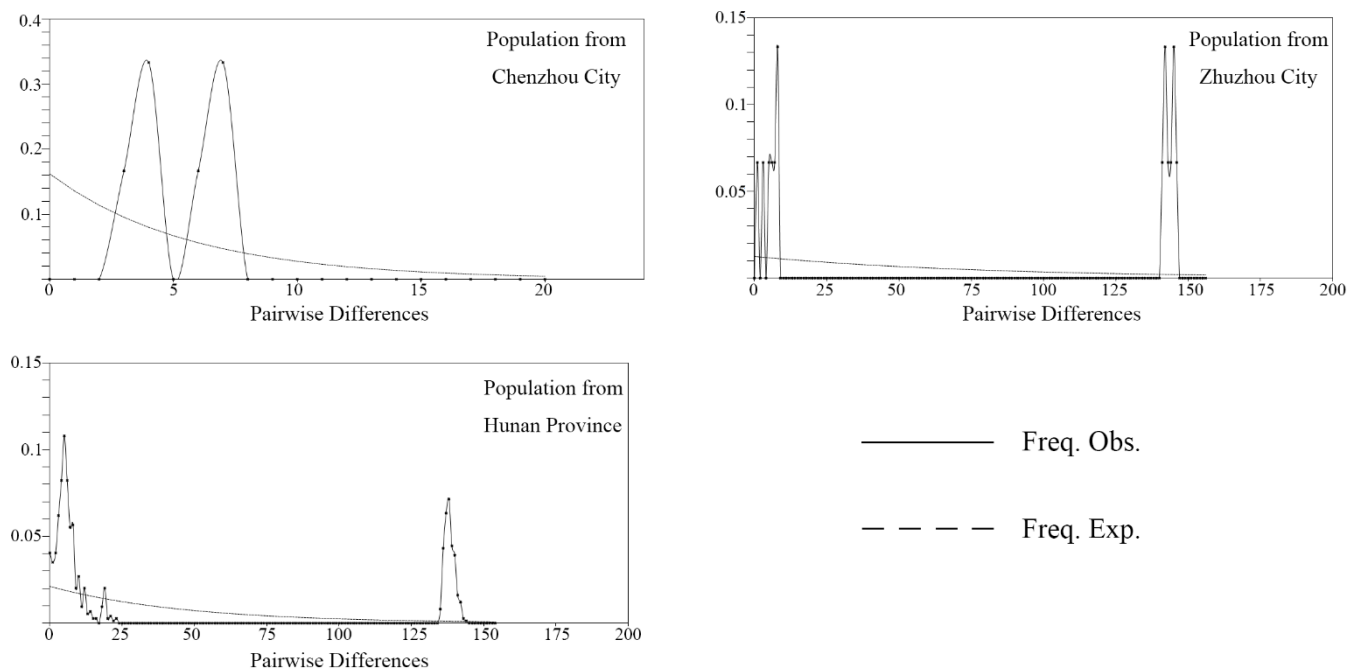


Figure 5. Maps of the mismatch distribution of population from seven cities in Hunan Province, based on mitochondrial genes COI + COII + 12S + 16S + ND1. The abscissa represents the number of pairwise distances. The ordinate represents the number of observations. The lines represent the expected (dashed) and observed (smoothed) frequencies of pairwise differences under sudden lineage expansion.

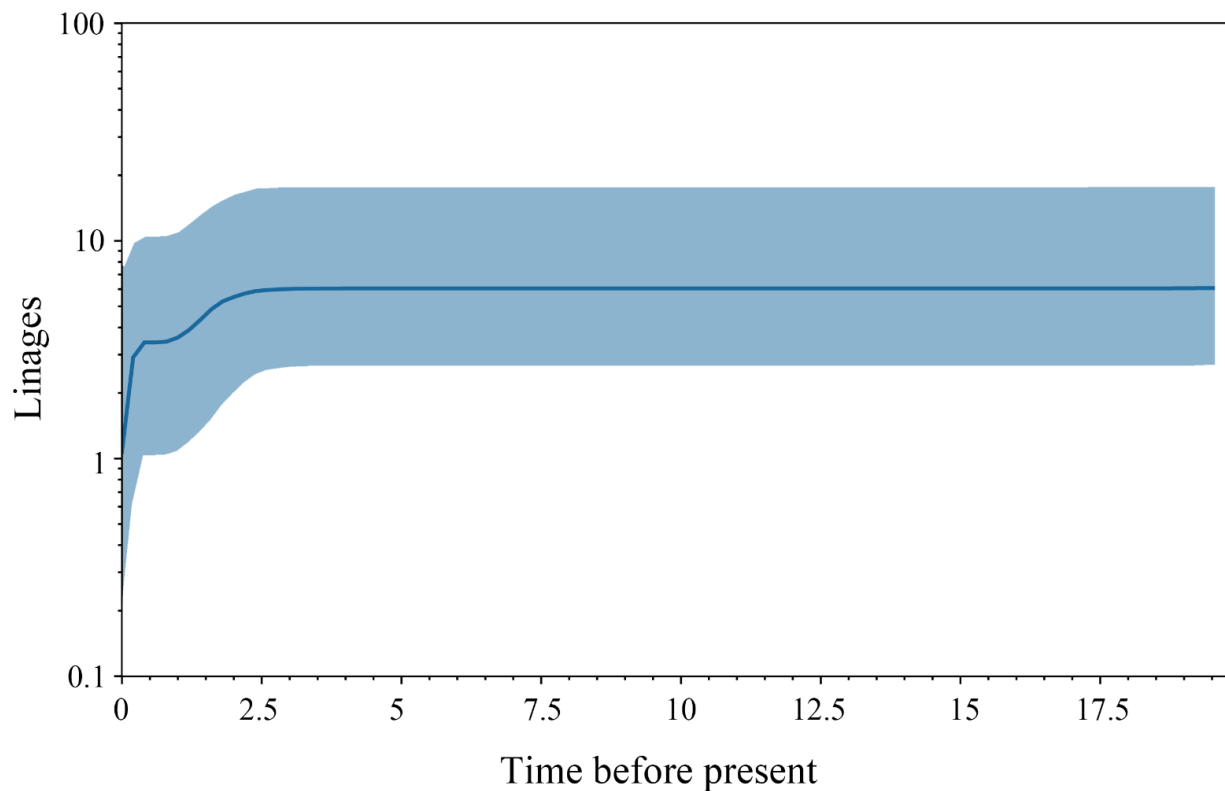


Figure 6. Bayesian skyline diagram of the population dynamic for populations of *M. remanens*. The areas shaded in light blue are within the 95% of highest posterior density interval. The dotted vertical lines indicate the important population size changes of *M. remanens*.

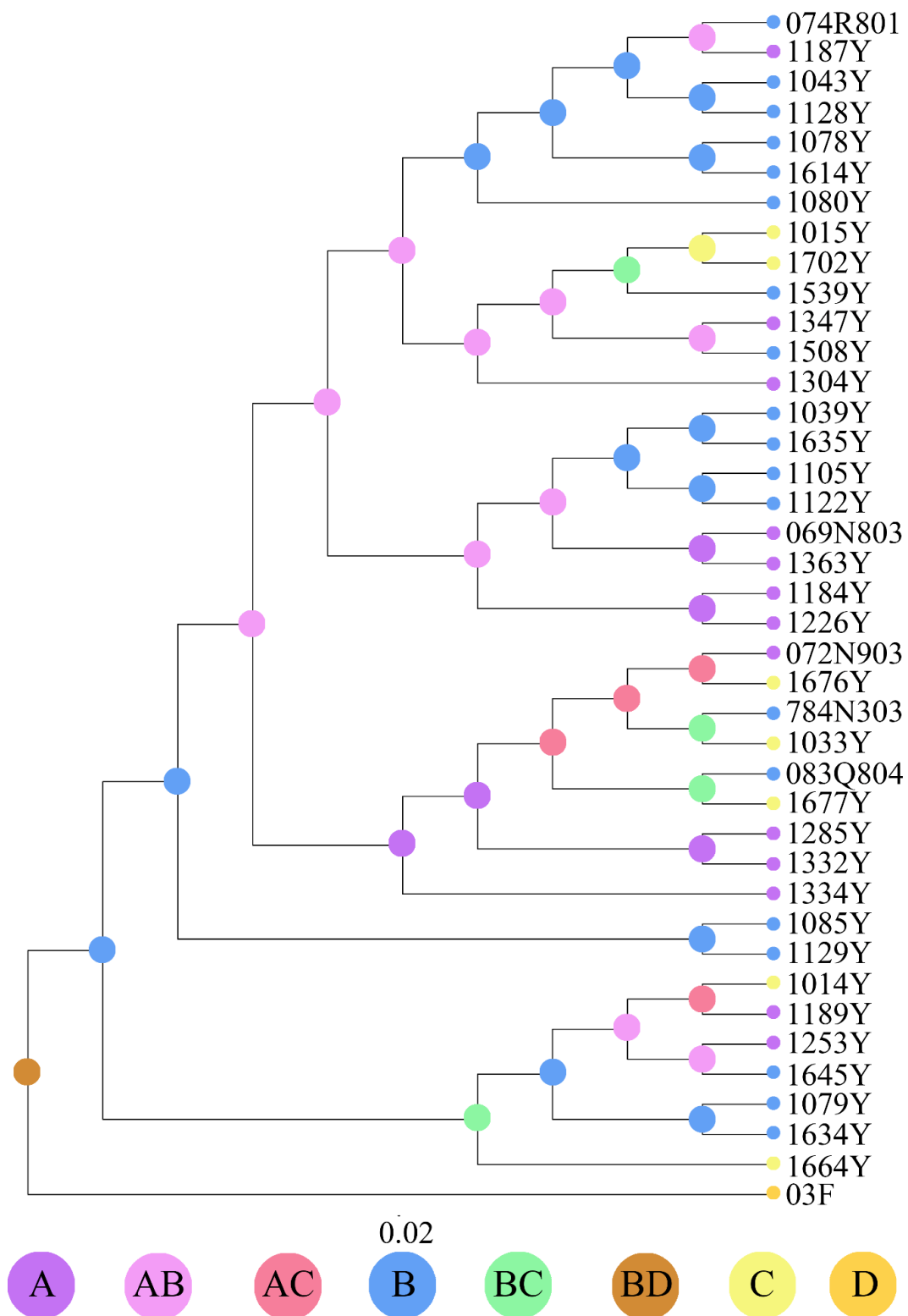


Figure 7. Distribution map of the ancestral region of *M. remanens*. Region A represents Yongzhou and Chenzhou cities; Region B represents Hengyang, Zhuzhou, and Xiangtan cities; Region C represents Changsha and Yueyang cities; Region D represents Shanghai cities; Region AB represents combination of Region A and Region B; Region AC represents combination of Region A and Region C; Region BC represents combination of Region B and Region C; Region BD represents combination of Region B and Region D.

4. Discussion

Parthenogenesis refers to the reproductive mode in which the ovum develops into completely new individuals without fertilization. In general, loss of sexual reproduction hinders biological evolution [33,34]. However, earthworms exhibit parthenogenesis and are mainly concentrated in the Megascolecidae and Lumbricidae families [3]. The combination of parthenogenetic strategies and chromosomal polyploidy greatly increases the heterozygosity level of earthworm taxa, which is beneficial for resisting environmental stress and adapting to a wide range of extreme environments [35]. Parthenogenesis usually leads to polymorphism in earthworms, with morphological variability related mainly to the reduction of reproductive structures, such as spermathecae, prostates, seminal vesicles, and an empty seminal chamber [35–47]. *M. remanens* has a tendency toward parthenogenesis, with a lack of male pores, degeneration of prostate glands, and loss of seminal vesicles.

Haplotype diversity (Hd) and nucleotide diversity (Pi) are commonly used as evaluation indices, in order to assess the genetic diversity of a population [38]. The population from Hunan Province showed high genetic diversity (Pi: 0.01366, Hd: 0.960), except in Xiangtan and Chenzhou cities, suggesting that the population evolved over a long period to produce a large and stable population in most areas. The population from Xiangtan and Chenzhou cities showed characteristics of low genetic diversity, which may be related to the number of research samples. High haplotyp and nucleotide diversity may be caused by the existence of two differentiated lineages, or two contacts, between independent populations in the species, or the population presents a stable and growing model and does not experience a bottleneck effect or population expansion [39]. Combined with the dynamics of *M. remanens*, its high genetic diversity may also be related to the environmental heterogeneity of the population or physiological characteristics of population life [40]. The distribution and morphological characteristics of the species are the result of long-term natural selection and evolution in a specific ecological environment. This demonstrates the adaptability of this species to the environment. It is generally believed that high genetic diversity indicates that the species has strong adaptability to environmental changes [40]. Therefore, it is speculated that the complex and changeable environment led to the degradation of the morphological structure of *M. remanens*, but their genetic diversity was not greatly reduced, making it adaptable to extreme environments and conducive to survival [41].

In addition to the population collected from Xiangtan City, the neutral test and mismatch distribution map showed no population expansion of *M. remanens* in Hunan Province. The results showed that the population size has remained stable in recent years, and there has been no significant population expansion. This may be related to the mode of parthenogenetic reproduction and environment.

The root of the tree, corresponding to the diversification of *M. remanens* and *A. pectiniferus*, coincides with the Quaternary glacial period (2.58 Ma) [42]. BSP analysis indicated that the Quaternary ice age had an impact on the diffusion of *M. remanens*, and there should have been several refuges during this period [43]. The Quaternary glaciation has led to repeated and drastic environmental changes [44–46]. It profoundly shapes the current distribution and genetic structure of many animal and plant species in the temperate zone of the Northern Hemisphere. The last Quaternary ice age ended with a recession event, from 0.015 to 0.01 Ma, in the middle latitudes [47]. The geographical distribution pattern of *M. remanens* was formed at approximately 0.0074 Ma, and its diffusion process was completely covered by Quaternary ice. The Quaternary glacial period may be an important factor that accelerated the differentiation and colonization of *M. remanens*. The colonization routes of *M. remanens* were from south to north in Hunan Province. This is consistent with the dispersal direction of earthworms in China [48,49]. The species in Region A may be affected by environmental and biological factors, such as human activity.

In summary, ancient geographical events, climate change, geographical isolation (islands, oceans, and rivers), environmental factors, and human activity may play an important role in the differentiation and diffusion of *M. remanens*.

5. Conclusions

Metaphire remanens sp. nov. (Oligochaeta: Megascolecidae) is an endemic earthworm species that is widely distributed in Hunan Province. Based on the existing samples and genetic data, the genetic structure of the population shows a high degree of isolation. Distinguishing genetic differentiation occurs in several cities. All populations had high haplotype and nucleotide diversity, except in Xiangtan and Chenzhou cities. With the exception of Xiangtan City, the other population did not experience expansion. This may be related to its evolution toward parthenogenesis. These results indicate that the populations of *M. remanens* stabilized after a long period of evolution. Glaciation, geographic isolation, and dispersal ability may be the major factors that promote the colonization of *M. remanens*. In the future, we will explore more samples of *M. remanens*, in order to supplement intermediate mutation samples. This lays the foundation for the study of the differentiation, dispersal, and parthenogenesis of *M. remanens*, including additional populations, based on the results of this study.

6. Description of *Metaphire remanens* sp. nov.

Taxonomy

Family Megascolecidae Rosa, 1891

Genus *Metaphire* Sims and Easton, 1972

Material examined. Holotype, 1 clitellates (P1CJHUSH190521800 N5-04A): China, Hunan Province, Chenzhou City (26°10'1" N, 113°7'30" E), 92 m elevation, brown soil under weed in vegetable garden, 21 May 2019, J.B. Jiang, J.L. Li, and Y. Wang. Paratypes, 122 clitellates in total: 1 clitellates (P1CJHUSH190521800 N5-04B): China, Hunan Province, Chenzhou City (26°10'1" N, 113°7'30" E), 92 m elevation, brown soil under weed in vegetable garden, 21 May 2019, J.B. Jiang, J.L. Li, and Y. Wang. Eight clitellates (P1CJHUSH190510089 N5-01): China, Hunan Province, Changsha City (28°5'9" N, 112°47'2" E), 47 m elevation, brown soil under weed in farmland, 10 May 2019, J.B. Jiang, J.L. Li, and B.Y. Yin. One clitellates (P1CJHUSH190510089 N5-02): China, Hunan Province, Changsha City (28°5'9" N, 112°47'2" E), 47 m elevation, brown soil under weed in farmland, 10 May 2019, J.B. Jiang, J.L. Li, and B.Y. Yin. One clitellates (P1CJHUSH190528089 N9-04): China, Hunan Province, Changsha City (28°5'38" N, 113°6'7" E), 24 m elevation, brown soil under weed in farmland, 28 May 2019, J.B. Jiang, J.L. Li, and Y. Wang. Two clitellates (P1CJHUSH190510779 N4-04): China, Hunan Province, Changsha City (28°16'59" N, 113°43'33" E), 70.65 m elevation, yellow soil under crops in farmland, 10 May 2019, Y. Dong, Y.F. Qin, and Y.Z. Wu. Four clitellates (P1CJHUSH190511779 N9-01): China, Hunan Province, Changsha City (28°19'40" N, 113°31'12" E), 112.45 m elevation, red soil under vegetable in vegetable garden, 11 May 2019, Y. Dong, Y.F. Qin, and Y.Z. Wu. One clitellates (P1CJHUSH190511779 N9-02): China, Hunan Province, Changsha City (28°19'40" N, 113°31'12" E), 112.45 m elevation, red soil under vegetable in vegetable garden, 11 May 2019, Y. Dong, Y.F. Qin, and Y.Z. Wu. One clitellates (P1CJHUSH190510083 N1-04): China, Hunan Province, Xiangtan City (28°58'58" N, 112°48'57" E), 47 m elevation, brownish yellow soil under shrub in farmland, 10 May 2019, J.B. Jiang, J.L. Li, and B.Y. Yin. Three clitellates (P1CJHUSH190510083 N1-08): China, Hunan Province, Xiangtan City (28°58'58" N, 112°48'57" E), 47 m elevation, brownish yellow soil under shrub in farmland, 10 May 2019, J.B. Jiang, J.L. Li, and B.Y. Yin. Six clitellates (P1CJHUSH190511083 Q8-04): China, Hunan Province, Xiangtan City (27°34'4" N, 112°40'51" E), 88 m elevation, brown soil under weed at roadside, 11 May 2019, J.B. Jiang, J.L. Li, and B.Y. Yin. Four clitellates (P1CJHUSH190512778 Q9-03): China, Hunan Province, Yueyang city (28°51'24" N, 113°36'33" E), 178.15 m elevation, yellow soil under weed at roadside, 12 May 2019, Y. Dong, Y.F. Qin, and Y.Z. Wu. One clitellates (P1CJHUSH190512079 N3-01): China, Hunan Province, Hengyang City (27°6'46" N, 112°34'58" E), 110 m elevation, brown soil under weed in dry farmland, 12 May 2019, J.B. Jiang, J.L. Li, and B.Y. Yin. One clitellates (P1CJHUSH190512784 N4-04): China, Hunan Province, Hengyang City (27°17'56" N, 112°49'4" E), 67 m elevation, brown soil under weed in dry farmland, 12 May 2019, J.B. Jiang, J.L. Li, and B.Y. Yin. Four clitellates (P1CJHUSH190512784 N4-

05): China, Hunan Province, Hengyang City (27°17'56" N, 112°49'4" E), 67 m elevation, brown soil under weed in dry farmland, 12 May 2019, J.B. Jiang, J.L. Li, and B.Y. Yin. Sixteen clitellates (P1CJHUSH190512784 N5-01): China, Hunan Province, Hengyang City (27°20'45" N, 112°46'48" E), 114 m elevation, brown soil under weed in dry farmland, 12 May 2019, J.B. Jiang, J.L. Li, and B.Y. Yin. One clitellates (P1CJHUSH190512784 R7-05): China, Hunan Province, Hengyang City (27°23'42" N, 112°40'8" E), 88 m elevation, brownish red soil under bamboo in woodland, 12 May 2019, J.B. Jiang, J.L. Li, and B.Y. Yin. Three clitellates (P1CJHUSH190512784 N3-03): China, Hunan Province, Hengyang City (27°14'45" N, 112°48'54" E), 96 m elevation, brown soil under weed in dry farmland, 12 May 2019, J.B. Jiang, J.L. Li, and B.Y. Yin. One clitellates (P1CJHUSH190513074 N1-05): China, Hunan Province, Hengyang City (26°43'15" N, 112°35'5" E), 60 m elevation, brown soil under weed in dry farmland, 13 May 2019, J.B. Jiang, J.L. Li, and B.Y. Yin. Six clitellates (P1CJHUSH190513074 Q5-03): China, Hunan Province, Hengyang City (26°36'3" N, 112°22'19" E), 88 m elevation, brown soil at roadside, 13 May 2019, J.B. Jiang, J.L. Li, and B.Y. Yin. One clitellates (P1CJHUSH190513074 Q5-05): China, Hunan Province, Hengyang City (26°36'3" N, 112°22'19" E), 88 m elevation, brown soil at roadside, 13 May 2019, J.B. Jiang, J.L. Li, and B.Y. Yin. Eight clitellates (P1CJHUSH190513074 R8-01): China, Hunan Province, Hengyang City (26°51'7" N, 112°16'19" E), 106 m elevation, brownish red soil under bamboo in woodland, 13 May 2019, J.B. Jiang, J.L. Li, and B.Y. Yin. One clitellates (P1CJHUSH190515072 N4-04): China, Hunan Province, Yongzhou City (26°28'58" N, 111°39'39" E), 107 m elevation, brown soil under weed in dry farmland, 15 May 2019, J.B. Jiang, J.L. Li, and B.Y. Yin. One clitellates (P1CJHUSH190516072 Q6-01): China, Hunan Province, Yongzhou City (26°21'10" N, 111°37'30" E), 116 m elevation, brown soil under weed beside pond, 16 May 2019, J.B. Jiang, J.L. Li, and B.Y. Yin. Twelve clitellates (P1CJHUSH190516072 Q8-01): China, Hunan Province, Yongzhou City (26°16'58" N, 111°41'27" E), 129 m elevation, brown soil under mulberries in orchard, 16 May 2019, J.B. Jiang, J.L. Li, and B.Y. Yin. Four clitellates (P1CJHUSH190516072 N9-03): China, Hunan Province, Yongzhou City (26°15'7" N, 111°40'26" E), 117 m elevation, brown soil under weed in dry farmland, 16 May 2019, J.B. Jiang, J.L. Li, and B.Y. Yin. Three clitellates (P1CJHUSH190517069 N4-01): China, Hunan Province, Yongzhou City (25°10'22" N, 111°37'1" E), 219 m elevation, brown soil under weed in dry farmland, 17 May 2019, J.B. Jiang, J.L. Li, and B.Y. Yin. One clitellates (P1CJHUSH190517069 N8-03): China, Hunan Province, Yongzhou City (25°18'3" N, 111°38'2" E), 201 m elevation, brown soil under weed in dry farmland, 17 May 2019, J.B. Jiang, J.L. Li, and B.Y. Yin. One clitellates (P1CJHUSH190519808 R2-02): China, Hunan Province, Yongzhou City (25°45'10" N, 112°18'36" E), 204 m elevation, brown soil under masson pine in woodland, 19 May 2019, J.B. Jiang, J.L. Li, and B.Y. Yin. One clitellates (P1CJHUSH190519808 Q7-05): China, Hunan Province, Yongzhou City (25°57'3" N, 112°15'28" E), 230 m elevation, brownish yellow soil under weed at roadside, 19 May 2019, J.B. Jiang, J.L. Li, and Y. Wang. One clitellates (P1CJHUSH190520798 N9-03): China, Hunan Province, Chenzhou City (25°59'49" N, 113°0'28" E), 90 m elevation, brown soil under weed in vegetable garden, 20 May 2019, J.B. Jiang, J.L. Li, and Y. Wang. One clitellates (P1CJHUSH190520798 Q10-01): China, Hunan Province, Chenzhou City (26°0'53" N, 112°59'16" E), 106 m elevation, brown soil under grass in lawn, 20 May 2019, J.B. Jiang, J.L. Li, and Y. Wang. One clitellates (P1CJHUSH190521799 N1-03): China, Hunan Province, Chenzhou City (26°24' N, 112°53'49" E), 259 m elevation, brown soil under weed in farmland, 21 May 2019, J.B. Jiang, J.L. Li, and Y. Wang. Two clitellates (P1CJHUSH190518807 N4-02B): China, Hunan Province, Yongzhou City (25°23'52" N, 112°13'37" E), 258 m elevation, brown soil under weed in dry farmland, 18 May 2019, J.B. Jiang, J.L. Li, and B.Y. Yin. One clitellates (P1CJHUSH190524073 N1-03): China, Hunan Province, Zhuzhou City (26°35'5" N, 113°35'52" E), 174 m elevation, brown soil under weed in farmland, 24 May 2019, J.B. Jiang, J.L. Li, and Y. Wang. One clitellates (P1CJHUSH190525780 Q2-01): China, Hunan Province, Zhuzhou City (27°0'46" N, 113°28'12" E), 151 m elevation, brown soil under withered grass at roadside, 25 May 2019, J.B. Jiang, J.L. Li, and Y. Wang. Two clitellates (P1CJHUSH190527082

Q1-01): China, Hunan Province, Zhuzhou City (27°50'31'' N, 113°20'49'' E), 82 m elevation, brown soil under weed at roadside, 27 May 2019, J.B. Jiang, J.L. Li, and Y. Wang. Four clitellates (P1CJHUSH190527082 N5-01): China, Hunan Province, Zhuzhou City (27°46'15'' N, 113°15'3'' E), 56 m elevation, brown soil under weed in farmland, 27 May 2019, J.B. Jiang, J.L. Li, and Y. Wang. Eight clitellates (P1CJHUSH190527082 N5-02): China, Hunan Province, Zhuzhou City (27°46'15'' N, 113°15'3'' E), 56 m elevation, brown soil under weed in farmland, 27 May 2019, J.B. Jiang, J.L. Li, and Y. Wang. 3 clitellates (P1CJHUSH190528082 N8-01): China, Hunan Province, Zhuzhou City (27°55'48'' N, 113°9'50'' E), 34 m elevation, brownish yellow soil under weed in vegetable garden, 28 May 2019, J.B. Jiang, J.L. Li, and Y. Wang.

Etymology

The species is named after its type characteristic.

Diagnosis

Size medium. Spermathecal pores in 6/7–7/8, 0.33 of body circumference, ventrally apart. Male pores one pair in XVIII, 0.33 of circumference, apart ventrally, each on the bottom center of the longitudinally distributed copulatory chamber, slightly raised (Figure 8A). Sometimes have no male pores (specimen: P1CJHUSH190518807 N4-02, P1CJHUSH190510089 N5-01, P1CJHUSH190516072 Q8-01, P1CJHUSH190528082 N8-01, P1CJHUSH190512784 N4-05, P1CJHUSH190527082 N5-01, and P1CJHUSH190510779 N4-04) (Figure 8B). Spermathecae, two pairs in VII and VIII, ampulla bag-shaped. Diverticulum as long as main pouch (duct and ampulla together), slender, terminal 1/3 dilated into bag-shaped seminal chamber. Sometimes no spermathecae (specimen: the same as above). Intestinal caeca are simple. Prostate glands degeneration (Figure 8).

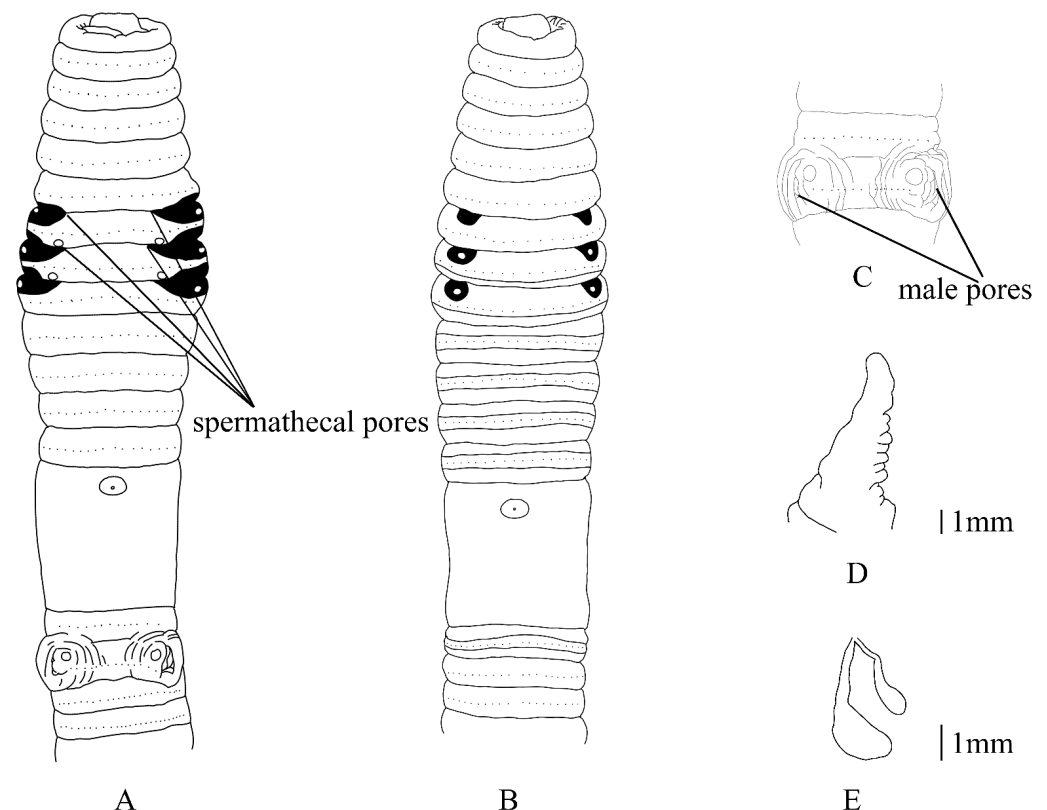


Figure 8. *Metaphire remanens* sp. nov. (A) ventral body surface with spermathecal pores and male pores; (B) ventral body surface with male pores of cryptic species; (C) intestinal caeca; (D) intestinal caeca; (E) spermathecae.

External characters

Light yellowish brown dorsal pigment, no pigment on ventral pigment. Dimensions 68–110 mm by 3.9–5.7 mm at clitellum, segments 88–98. No annulus, sometimes present on

VIII–XIII and XVII (specimen: P1CJHUSH190518807 N4-02). The dorsal midline is invisible. First dorsal pore in 10/11, sometimes in 12/13 (specimen: P1CJHUSH190518807 N4-02 and P1CJHUSH190510089 N5-01). Prostomium 1/2 epilobous. Clitellum annular, yellowish brown, in XIV–XVI, swollen, setae invisible externally, no dorsal pores. Setae numbering 34–40 at III, 38–44 at V, 44–48 at VIII, 52–62 at XX, 56–66 at XXV, 14–17 between male pores, 11–14 (VI), 12–15 (VII) between spermathecal pores, setal formula: aa = 1.0–1.6ab, zz = 1.2–2.2 zy. Spermathecal pores, two pairs in 6/7–7/8, ventral, invisible, 0.33 of body circumference, ventrally apart from each other. An obvious subsidence area on both sides of 6/7–8/9, 0.5 of body circumference, ventrally apart from each other. Sometimes the areas present on the left side of 5/6–7/8 and right side of 6/7–8/9, 0.5 of body circumference, ventrally apart from each other (specimen: P1CJHUSH190512079 N3-01). An oval, small-sized papilla near the subsidence area on both sides of 6/7. A total of 0–2 oval, small-sized papillae near the subsidence area on both sides of 7/8 and 8/9, respectively. Sometimes no papilla (specimen: P1CJHUSH190510089 N5-01 and P1CJHUSH190527082 N5-02). Female pore, single in XIV, ellipse, milky white. Male pores, one pair in XVIII, 0.33 of circumference apart ventrally, each on the bottom center of the longitudinally distributed copulatory chamber, slightly raised. A total of 0–3 oval medium-sized, flat-topped papillae on the cushion protrusion (Figure 8C). Sometimes no male pores (specimen: P1CJHUSH190518807 N4-02, P1CJHUSH190510089 N5-01, P1CJHUSH190516072 Q8-01, P1CJHUSH190528082 N8-01, P1CJHUSH190512784 N4-05, P1CJHUSH190527082 N5-01, and P1CJHUSH190510779 N4-04).

Internal characters

Septa 5/6–7/8 thick and muscular, 10/11–13/14 slightly thickened, 8/9 and 9/10 absent. Gizzard spherical, in IX–X. Intestine enlarged distinctly from XV. Intestinal caeca paired in XXVII, extending anteriorly to XXII, simple, smooth on dorsal side, 6–10 dentate sacs on ventral side (Figure 8D). Four esophageal hearts in X–XIII, the latter three are more developed than the first pair. Male sexual system holandric, no testis sacs. Seminal vesicles two pairs in XI–XII, not developed, left and right lobes separated on the ventral side. Sometimes, left and right lobes connected on the ventral side (specimen: P1CJHUSH190518807 N4-02, P1CJHUSH190510089 N5-01, P1CJHUSH190516072 Q8-01, P1CJHUSH190528082 N8-01, P1CJHUSH190512784 N4-05, P1CJHUSH190527082 N5-01, and P1CJHUSH190510779 N4-04). Left prostate glands degeneration, prostatic duct on XVIII, slightly thicker at the distal part. Right prostate glands not developed, inserting in XVIII and extending to 1/2 XVIII and 1/2 XX, prostatic duct U-shaped on XVIII, slightly thicker at the distal part. Sometimes, both sides degeneration (specimen P1CJHUSH190527082 N5-02, P1CJHUSH190512079 N3-01, P1CJHUSH190518807 N4-02, P1CJHUSH190510089 N5-01, P1CJHUSH190516072 Q8-01, P1CJHUSH190528082 N8-01, P1CJHUSH190512784 N4-05, P1CJHUSH190527082 N5-01, and P1CJHUSH190510779 N4-04). A total of 0–1 petiolate accessory gland on the left side, 0–1 petiolate accessory gland on the right side of XVII. A total of 0–2 petiolate accessory glands on the left side, 0–4 petiolate accessory glands on the right side of XVIII. A total of 0–1 petiolate accessory gland on the left side, 0–1 petiolate accessory gland on the right side of XIX. Spermathecae, two pairs in VII and VIII, ampulla bag-shaped, about 2.0–3.0 mm long in holotype; ampulla duct as long as or 1.5 times of ampulla. Diverticulum as long as main pouch (duct and ampulla together), slender, terminal 1/3 dilated into bag-shaped seminal chamber (Figure 8E). Sometimes no spermathecae (specimen P1CJHUSH190527082 N5-02, P1CJHUSH190512079 N3-01, P1CJHUSH190518807 N4-02, P1CJHUSH190510089 N5-01, P1CJHUSH190516072 Q8-01, P1CJHUSH190528082 N8-01, P1CJHUSH190512784 N4-05, P1CJHUSH190527082 N5-01 and P1CJHUSH190510779 N4-04). A total of 0–2 petiolate accessory glands on the left side, 0–4 petiolate accessory glands on the right side of VII. A total of 0–2 petiolate accessory glands on the left side, 0–4 petiolate accessory glands on the right side of VIII. A 0–1 petiolate accessory gland on the left side, 0–3 petiolate accessory glands on the right side of IX.

Remarks

Metaphire remanens sp. nov. can be assigned to the *Metaphire planata* species group characterized by having two spermathecal pores in 6/7–8/9 (Sims and Easton, 1972) [50]. To date, this species group contains nine species: *M. decipiens* (Beddard, 1912), *M. dunckeri* (Michaelson, 1902), *M. ferdinandi* (Michaelson, 1891), *M. parvula* (Ohfuchi, 1956), *M. planata* (Gates, 1926), *M. sintangi* (Michaelson, 1922), *M. jianfengensis* Quan 1985, *M. dadingmontis* Zhang 2006, and *M. saxicalcis* Bantaowong 2016.

Within the *M. planata*-group, *Metaphire remanens* sp. nov. is different from others, in that it has a smaller size, fewer setae, spermathecal pores with an obvious subsidence area, intestinal caeca paired in XXVII–XXII, no testis sacs, prostates glands degeneration, ampulla bag-shaped, and a diverticulum terminal 1/3 dilated into bag-shaped seminal chamber. Sometimes, no spermathecae. Among 123 individuals, 35 individuals have no male pores. The results of the pairwise distance of COI (6.0%–6.6%) and phylogenetic tree (Clade 5) indicated that it may be a cryptic species that requires further taxonomic research (Table 2, Figure 2).

Metaphire remanens sp. nov. is similar to *M. dadingmontis*, in terms of body size, setae, spermathecal pores, and male pores [51] (Table 4). However, the new species differs from *M. dadingmontis* in the clitellum with no dorsal pores, spermathecal pores with obvious subsidence areas, sometimes no male pores, thicker septa in 5/6–13/14, gizzard in IX–X, intestine enlarged from XV, intestinal in XXVII–XXII, no testis sacs, prostate glands degeneration, and spermathecae degeneration; *M. dadingmontis* clitellum with dorsal pores, thin septa, gizzard in VIII–X, intestine enlarged from XVI, intestinal in XXVII–XXIV, testis sacs in X and XI, and prostate glands developed.

Metaphire remanens sp. nov. is distinguished from *M. planata* by its smaller size, first dorsal pore in 10/11 or 12/13, clitellum with invisible setae, fewer setae, spermathecal pores with obvious subsidence areas, sometimes no male pores, septa, intestinal in XXVII–XXII, no testis sacs, and sometimes prostate gland and spermathecae degeneration; while *M. planata* first dorsal pore in 11/12, clitellum with visible setae, intestinal in XXVII–XXI, and testis sacs in X and XI [52] (Table 4).

Metaphire remanens sp. nov. is somewhat similar to *M. jianfengensis* by the first dorsal in 12/13, male pores, septa, gizzard in IX–X, and intestine enlarged from XV [53] (Table 4). However, the new species is characterized by smaller size, fewer setae, spermathecal pores with obvious subsidence areas, intestinal in XXVII–XXII, no testis sacs, sometimes prostate gland, and spermathecae degeneration, whereas *M. jianfengensis* is intestinal in XXVII–XXV, testis sacs in X and XI, and prostate gland in XVII–XIX.

Metaphire remanens sp. nov. differs from *M. saxicalcis* by its smaller size, fewer setae, spermathecal pores with obvious subsidence areas, sometimes no male pores, septa of 10/11–13/14 slightly thickened, no testis sacs, sometimes prostate gland, and spermathecae degeneration, whereas *M. saxicalcis* septa of 10/11–11/12 thin, testis sacs in X and XI, and prostate gland in XVII–XXI [52] (Table 4).

Besides, a phylogenetic tree between shows differences between *M. remanens* and some similar species of the *Metaphire* genus, i.e., *M. acincta*, *M. californica*, *M. communissima*, *M. guillelmi*, *M. yamadai*, *M. saxicalcis*, *M. vesiculata*, *M. vulgaris*, and *M. peguana*, from COI gene delimitation (Figure 9).

Table 4. Comparison of characteristics of *M. remanens* sp. nov., *M. planata*, *M. jianfengensis*, *M. dadingmontis*, and *M. saxicalcis*.

Character	<i>M. remanens</i> sp. nov.	<i>M. planata</i>	<i>M. jianfengensis</i>	<i>M. dadingmontis</i>	<i>M. saxicalcis</i>
Body size (mm)	68–110 × 3.9–5.7	125 × 4.8	160–250 × 6–10	80–85 × 2.9–3.4	254–377 × 9.6
Segments	88–98	138	131–173	82–90	147–157
First dorsal pore	10/11, 12/13	11/12	12/13	12/13	12/13
Clitellum	XIV–XVI, no dorsal pores	XIV–XVI, visible setae	XIV–XVI	XIV–XVI, dorsal pores	XIV–XVI

Table 4. Cont.

Character	<i>M. remanens</i> sp. nov.	<i>M. planata</i>	<i>M. jianfengensis</i>	<i>M. dadingmontis</i>	<i>M. saxicalcis</i>
Setae	34–40/III, 38–44/V, 44–48/VIII, 58–62/XX, 56–66/XXV; 14–17 between male pores; 11–14 (VI), 12–15 (VII) between spermathecal pores; aa = 1.0–1.6ab, zz = 1.2–2.2zy.	60–69/III, 75–87/VIII, 56–65/XX; 11 between male pores; aa = 1.0ab, zz = 1.0zy.	52–56/III, 58–60/V, 65–66/VIII, 82–84/XXV.	32–40/III, 30–36/V, 38–42/VIII, 40–44/XX, 43–46/XXV; 7–9 between male pores; aa = 1.1–1.2ab, zz = 1.0–1.2zy.	89–98/XX; 13–20 between male pores; aa = 1.0ab, zz = 1.0zy.
Spermathecal pores	Two pairs, 6/7–7/8, 0.33C; An obvious subsidence area; 0–5 papillae.	Two pairs, 6/7–7/8, 0.25C.	Two pairs, 6/7–7/8, 1/4C.	Two pairs, 6/7–7/8, 0.33C; 2 papillae.	Two pairs, 6/7–7/8.
Male pores	XVIII, 0.33C; Each on the bottom center of the longitudinally distributed copulatory chamber, slightly raised; 0–3 oval medium-sized flat-topped papillae on the cushion protrusion. Sometimes no male pores.	XVIII, 0.27C; transversely slit-like secondary apertures puckered radially around its margin.	XVIII, 0.25C; Each on the bottom center of the copulatory chamber; Two large-sized circular papillae and three small pads on the inner wall of the cavity are squeezed together to form a concave shape, surrounded by many longitudinal fold muscles; The mastoid is exposed when everted.	XVIII, 0.4C; each on the surface of a small protuberance situated in a large copulatory chamber in XVIII, surrounded by longitudinal epidermic folds. No papillae.	XVIII, 0.28C; secondary apertures transversely slit-like with puckered margin on segment XVIII, no genital markings.
Septa	5/6–7/8 thick and muscular, 10/11–13/14 slightly thickened, 8/9 and 9/10 absent.	6/7–7/8 muscular, 10/11–12/13 slightly muscular, 8/9–9/10 absent.	4/5–7/8 thick and muscular, 10/11–13/14 slightly thickened, 8/9 and 9/10 absent.	Thin, 8/9 and 9/10 absent.	5/6–7/8 thick, 10/11–11/12 thin, 8/9–9/10 absent.
Gizzard	IX–X, spherical	IX–X, spherical	IX–X	VIII–X, small and drum-like	Behind 7/8
Intestine	Enlarged from XV	Enlarged from XV	Enlarged from XV	Enlarged from XVI	Enlarged from XV
Intestinal caeca	XXVII–XXII	XXVII–XXI	XXVII–XXV	XXVII–XXIV	XXVII–XXII
Testis sacs	No.	Two pairs, X and XI.	Two pairs, X and XI, not developed.	Two pairs, X and XI.	Two pairs, X and XI.
Prostate glands	Left degeneration, right not developed/degeneration; 0–7 glands.	1/2 XVII–XIX, not developed.	XVII–XIX, developed; no glands.	XVIII, moderately large, prostatic duct simple curved. two glands.	XVI–XXI, developed.
Spermathecae	Two pairs, VII and VIII; Ampulla bag-shaped, ampulla duct as long as or 1.5 times of ampulla; Diverticulum as long as main pouch, slender, terminal 1/3 dilated into bag-shaped seminal chamber. Sometimes no spermathecae. A total of 0–14 glands.	Two pairs, VII and VIII; Ampulla heart-shaped, ampulla duct 1/3 of ampulla. Diverticulum as long as main pouch, slender, terminal 1/3 dilated into club-shaped seminal chamber. Four glands.	Two pairs, VII and VIII; Ampulla oval, ampulla duct as long as ampulla; Diverticulum shorter than main pouch, curved, terminal 1/4 dilated into seminal chamber.	Two pairs, VII–VIII; ampulla small oval-shaped, ampulla duct 1/4 of ampulla. Diverticulum as long as the whole spermatheca, slender, terminal 1/5 dilated into oval seminal chamber. Has glands.	Two pairs, VII and VIII; ampulla paddle-shaped, ampulla duct 1/3 of ampulla. Diverticulum longer than main pouch, slender, terminal 1/4 dilated into seminal chamber.

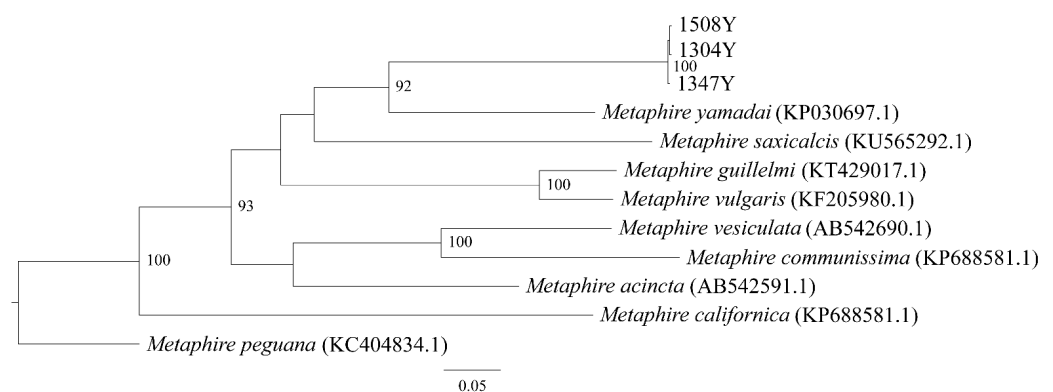


Figure 9. Phylogenetic tree, reconstructed using Bayesian phylogeny estimation, based on COI gene. Bayesian posterior probabilities ($pp \geq 0.95$) are shown on the branches. Numbers in parentheses are GenBank accession numbers.

Author Contributions: Conceptualization, Q.J., J.J., and J.Q.; data curation, Q.J. and J.J.; formal analysis, Q.J.; investigation, Q.J., J.J., and J.L.; writing—original draft, Q.J. and J.Q.; writing—review and editing, Q.J. and J.Q. All authors have read and agreed to the published version of the manuscript.

Funding: This research was funded by the National Science Foundation of China grant (no. 42077028, 41701272) and National Science and Technology Fundamental Resources Investigation Program of China (2018FY100300).

Institutional Review Board Statement: Not applicable.

Informed Consent Statement: Not applicable.

Data Availability Statement: DNA sequences: GenBank accession No. AB542591.1 for *Metaphire acincta*, KP688581.1 for *Metaphire californica*, AB542623.1 for *Metaphire communissima*, KT429017.1 for *Metaphire guillelmi*, KP030697.1 for *Metaphire yamadai*, KU565292.1 for *Metaphire saxicalcis*, AB542690.1 for *Metaphire vesiculate*, KF205980.1 for *Metaphire vulgaris*, and KC404834.1 for *Metaphire peguana*.

Acknowledgments: We are grateful to Yan Dong, Yifeng Qin, Yizhao Wu, Yue Wang, and Bangyi Yin for their assistance with the field work.

Conflicts of Interest: The authors declare no conflict of interest.

References

1. Thakuria, D.; Schmidt, O.; Finan, D.; Egan, D.; Doohan, F.M. Gut Wall Bacteria of Earthworms: A natural Selection Process. *ISME J.* **2010**, *4*, 357–366. [[CrossRef](#)] [[PubMed](#)]
2. Groffman, P.M.; Fahey, T.J.; Fisk, M.C.; Yavitt, J.B.; Sherman, R.E.; Bohlen, P.J.; Maerz, J.C. Earthworms Increase Soil Microbial Biomass Carrying Capacity and Nitrogen Retention in Northern Hardwood Forests. *Soil Biol. Biochem.* **2015**, *87*, 51–58. [[CrossRef](#)]
3. Sun, J.; James, S.W.; Jiang, J.; Yao, B.; Zhang, L.; Liu, M.; Qiu, J.; Hu, F. Phylogenetic Evaluation of *Amyntas* Earthworms from South China Reveals the Initial Ancestral State of Spermataceae. *Mol. Phylogenet. Evol.* **2017**, *115*, 106–114. [[CrossRef](#)] [[PubMed](#)]
4. De Sosa, I.; Marchán, D.F.; Novo, M.; Díaz Cosin, D.J.; Giribet, G.; Fernández, R. Insights into the Origin of parthenogenesis in Oligochaetes: Strong Genetic Structure in a Cosmopolitan Earthworm is Not Related to Reproductive Mode. *Eur. J. Soil Biol.* **2017**, *81*, 31–38. [[CrossRef](#)]
5. Shen, H.; Yu, H.; Chen, J. Parthenogenesis in Two Taiwanese Mountain Earthworms *Amyntas catenus* Tsai et al., 2001 and *Amyntas hohuanmontis* Tsai et al., 2002 (Oligochaeta, Megascolecidae) revealed by AFLP. *Eur. J. Soil Biol.* **2012**, *51*, 30–36. [[CrossRef](#)]
6. Real, F.M.; Haas, S.A.; Franchini, P.; Xiong, P.; Simakov, O.; Kuhl, H.; Schöpflin, R.; Heller, D.; Moeinzadeh, M.H. The Mole Genome Reveals Regulatory Rearrangements Associated with Adaptive Intersexuality. *Science* **2020**, *370*, 208–214. [[CrossRef](#)]
7. Lo, E.Y.Y.; Stefanović, S.; Dickinson, T.A. Geographical Parthenogenesis in Pacific Northwest Hawthorns (*Crataegus*; *Rosaceae*). *Botany* **2013**, *91*, 107–116. [[CrossRef](#)]
8. Jared, C.; Alexandre, C.; Mailho-Fontana, P.L.; Pimenta, D.C.; Brodie, E.D.; Antoniazzi, M.M. Toads Prey upon Scorpions and are Resistant to Their Venom: A biological and Ecological Approach to Scorpionism. *Toxicon* **2020**, *178*, 4–7. [[CrossRef](#)]
9. Kellner, K.; Seal, J.N.; Heinze, J. Sex at the Margins: Parthenogenesis vs. Facultative and Obligate Sex in a Neotropical Ant. *J. Evol. Biol.* **2013**, *26*, 108–117. [[CrossRef](#)]
10. Jiang, J.B. Taxonomy and Phylogeny of the Family Megascolecidae Earthworm from China. Ph.D. Thesis, Shanghai Jiao Tong University, Shanghai, China, 2016. (In Chinese).
11. Minamiya, Y.; Yokoyama, J.; Fukuda, T. A Phylogeographic Study of the Japanese Earthworm, *Metaphire sieboldi* (Horst, 1883) (Oligochaeta: Megascolecidae): Inferences from Mitochondrial DNA Sequences. *Eur. J. Soil Biol.* **2009**, *45*, 423–430. [[CrossRef](#)]
12. Zhang, Y.F.; Zhang, D.H.; Xu, Y.L.; Zhang, G.S.; Sun, Z.J. Effects of Fragmentation on Genetic Variation in Populations of the Terrestrial Earthworm *Drawida japonica* Michaelsen, 1892 (*Oligochaeta*, *Moniligastridae*) in Shandong and Liaodong peninsulas, China. *J. Nat. Hist.* **2012**, *46*, 1387–1405. [[CrossRef](#)]
13. Aspe, N.M.; James, S.W. Molecular Phylogeny and Biogeographic Distribution of Pheretimid Earthworms (*clitellata*: *Megascolecidae*) of the Philippine Archipelago. *Eur. J. Soil Biol.* **2018**, *85*, 89–97. [[CrossRef](#)]
14. Novo, M.; Almodovar, A.; Fernandez, R.; Giribet, G.; Cosin, D.J.D. Understanding the Biogeography of a Group of Earthworms in the Mediterranean Basin-The phylogenetic puzzle of *Hormogastridae* (*Clitellata*: *Oligochaeta*). *Mol. Phylogenet. Evol.* **2011**, *61*, 125–135. [[CrossRef](#)] [[PubMed](#)]
15. Dupont, L.; Gresille, Y.; Richard, B.; Decaens, T.; Mathieu, J. Dispersal Constraints and Fine-Scale Spatial Genetic Structure in Two Earthworm Species. *Biol. J. Linn. Soc.* **2015**, *114*, 335–347. [[CrossRef](#)]
16. Arbogast, B.S. Phylogeography: The history and Formation of Species. *Am. Zool.* **2001**, *41*, 134–135. [[CrossRef](#)]
17. Pop, A.A.; Wink, M.; Pop, V.V. Use of 18S, 16S rDNA and Cytochrome C Oxidase Sequences in Earthworm Taxonomy (*Oligochaeta*, *Lumbricidae*). *Pedobiologia* **2003**, *47*, 428–433. [[CrossRef](#)]
18. Folmer, O.; Black, M.; Hoeh, W.; Lutz, R.; Vrijenhoek, R. DNA Primers for Amplification of Mitochondrial Cytochrome C Oxidase Subunit I from Diverse Metazoan Invertebrates. *Mol. Mar. Biol. Biotechnol.* **1994**, *3*, 294–299.

19. Bely, A.E.; Wray, G.A. Molecular Phylogeny of Naidid Worms (*Annelida: Clitellata*) Based on Cytochrome Oxidase I. *Mol. Phylogenet. Evol.* **2004**, *30*, 50–63. [[CrossRef](#)]
20. Perez-Losada, M.; Ricoy, M.; Marshall, J.C.; Dominguez, J. Phylogenetic Assessment of the Earthworm *Aporrectodea caliginosa* species complex (*Oligochaeta: Lumbricidae*) Based on Mitochondrial and Nuclear DNA Sequences. *Mol. Phylogenet. Evol.* **2009**, *52*, 293–302. [[CrossRef](#)]
21. Hillis, D.M.; Mable, B.K.; Larson, A.; Davis, S.K.; Zimmer, E.A. Nucleic acids, IV: Sequencing and Cloning. In *Molecular Systematics*, 2nd ed.; Hillis, D.M., Moritz, C., Mable, B.K., Eds.; Sinauer Associates, Inc.: Massachusetts, MA, USA, 1996; pp. 321–381.
22. Darriba, D.; Taboada, G.L.; Doallo, R.; Posada, D. jModelTest 2: More Models, New Heuristics and Parallel Computing. *Nat. Methods* **2012**, *9*, 772. [[CrossRef](#)]
23. Ronquist, F.; Teslenko, M.; van der Mark, P.; Ayres, D.L.; Darling, A.; Höhna, S.; Larget, B.; Liu, L.; Suchard, M.A.; Huelsenbeck, J.P. MrBayes 3.2: Efficient Bayesian Phylogenetic Inference and Model Choice across a Large Model Space. *Syst. Biol.* **2012**, *61*, 539–542. [[CrossRef](#)] [[PubMed](#)]
24. Excoffier, L.; Laval, G.; Schneider, S. Arlequin ver. 3.0: An Integrated Software Package for Population Genetics Data Analysis. *Evol. Bioinform.* **2005**, *1*, 47–50. [[CrossRef](#)]
25. Leigh, J.W.; Bryant, D. PopART: Full-Feature Software for Haplotype Network Construction. *Methods. Ecol. Evol.* **2015**, *6*, 9. [[CrossRef](#)]
26. Librado, P.; Rozas, J. DnaSP v5: A Software for Comprehensive Analysis of DNA Poly-Morphism Data. *Bioinformatics* **2009**, *25*, 1451–1452. [[CrossRef](#)]
27. Tajima, F. Statistical Method for Testing the Neutral Mutation Hypothesis by DNA Polymorphisms. *Genetics* **1989**, *123*, 585–595. [[CrossRef](#)]
28. Fu, Y.X. Statistical Tests of Neutrality of Mutations Against Population Growth, Hitchhiking and Background Selection. *Genetics* **1997**, *147*, 915–925. [[CrossRef](#)]
29. Drummond, A.J.; Suchard, M.A.; Xie, D.; Rambaut, A. Bayesian Phylogenetics with BEAUti and the BEAST 1.7. *Mol. Biol. Evol.* **2012**, *29*, 1969–1973. [[CrossRef](#)]
30. Rambaut, A.; Drummond, A.J.; Dong, X.; Baele, G.; Suchard, M.A. Posterior Summarization in Bayesian Phylogenetics Using Tracer 1.7. *Syst. Biol.* **2018**, *67*, 901–904. [[CrossRef](#)]
31. Pérez, L.M.; Breinholt, J.W.; Porto, P.G.; Aira, M.; Domínguez, J. An Earthworm Riddle: Systematics and Phylogeography of the Spanish Lumbricid *Postandrilus*. *PLoS ONE* **2011**, *6*, e28153. [[CrossRef](#)]
32. Boore, J.L.; Brown, W.M. Complete DNA Sequence of the Mitochondrial Genome of the Annelid Worm *Lumbricus Terrestris*. *Genet. Mol. Res.* **1995**, *141*, 305–319.
33. Welch, D.M.; Meselson, M. Evidence for the Evolution of Bdelloid Rotifers without Sexual Reproduction or Genetic Exchange. *Science* **2000**, *288*, 1211–1215. [[CrossRef](#)] [[PubMed](#)]
34. Graham, B. *The Masterpiece of Nature: The Evolution and Genetics of Sexuality*; University of California Press: California, CA, USA, 1982; p. 635.
35. Cosín, D.J.D.; Novo, M.; Fernández, R. Reproduction of earthworms: Sexual selection and parthenogenesis. In *Biology of Earthworms*; Springer: Berlin/Heidelberg, Germany, 2011.
36. Gates, G. Contributions to North American earthworms. No. 3. IV. The trapezoides species group. *Bull. Tall Timbers Res. Stn.* **1972**, *12*, 146.
37. Qiu, J.; Bouché, M. Contribution to the taxonomy of Hormogastridae (*Annelida: Oligochaeta*) with Description of New Species from Spain. *Doc. Pedozool. Integrol.* **1998**, *4*, 164–177.
38. Bonin, A.; Nicole, F.; Pompanon, F.; Miaud, C.; Taberlet, P. Population Adaptive Index: A New Method to Help Measure Intraspecific Genetic Diversity and Prioritize Populations for Conservation. *Conserv. Biol.* **2007**, *21*, 697–708. [[CrossRef](#)] [[PubMed](#)]
39. Grant, W.A.S.; Bowen, B.W. Shallow Population Histories in Deep Evolutionary Lineages of Marine Fishes: Insights from Sardines and Anchovies and Lessons for Conservation. *J. Hered.* **1998**, *89*, 415–426. [[CrossRef](#)]
40. Nei, M. *Molecular Evolutionary Genetics*; Columbia University Press: New York, NY, USA, 1987; pp. 92–145.
41. Christensen, B. Asexual Propagation and Reproductive Strategies in Aquatic Oligochaeta. *Hydrobiologia* **1984**, *115*, 91–95. [[CrossRef](#)]
42. Head, M.J.; Gibbard, P.L. Formal Subdivision of the Quaternary System/Period: Past, Present, and Future. *Quat. Int.* **2015**, *383*, 4–35. [[CrossRef](#)]
43. Dong, Y.; Jiang, J.B.; Yuan, Z.; Zhao, Q.; Qiu, J.P. Population Genetic Structure Reveals Two Lineages of *Amyntas triastriatus* (*Oligochaeta: Megascolecidae*) in China, With Notes on a New Subspecies of *Amyntas triastriatus*. *Int. J. Environ. Res. Public Health* **2020**, *17*, 1538. [[CrossRef](#)]
44. Hewitt, G.M. Genetic Consequences of Climatic Oscillations in the Quaternary. *Philos. Tans. R. Soc. Lond. B Biol. Sci.* **2004**, *359*, 183–195. [[CrossRef](#)]
45. Qiu, Y.X.; Fu, C.X.; Comes, H.P. Plant Molecular Phylogeography in China and Adjacent Regions: Tracing the Genetic Imprints of Quaternary Climate and Environmental Change in the World’s Most Diverse Temperate Flora. *Mol. Phylogenet. Evol.* **2011**, *59*, 225–244. [[CrossRef](#)]

46. Ren, G.P.; Mateo, R.G.; Liu, J.Q.; Suchan, T.; Alvarez, N.; Guisan, A.; Conti, E.; Salamin, N. Genetic Consequences of Quaternary Climatic Oscillations in the Himalayas: *Primula Tibetica* as a Case Study Based on Restriction Site-Associated DNA Sequencing. *New Phytol.* **2017**, *213*, 1500–1512. [[CrossRef](#)] [[PubMed](#)]
47. Wright, H.E. Late Pleistocene climate of Europe: A review. *GSA Bull.* **1961**, *72*, 933–984. [[CrossRef](#)]
48. Jiang, J.B.; Qiu, J.P. Origin and Evolution of Earthworms Belonging to the Family *Megascolecidae* in China. *Biodivers. Sci.* **2018**, *26*, 1074–1082. [[CrossRef](#)]
49. Sun, J. Taxonomy and Molecular Phylogeny of *Amynthas* Earthworms from China. Ph.D. Thesis, Shanghai Jiao Tong University, Shanghai, China, 2013.
50. Sims, R.W.; Easton, E.G. A Numerical Revision of the Earthworm Genus *Pheretima auct* (Megascolecidae: Oligochaeta) with the Recognition of New Genera and an Appendix on the Earthworms Collected by the Royal Society North Borneo Expedition. *Biol. J. Linn. Soc.* **1972**, *4*, 169–268. [[CrossRef](#)]
51. Zhang, W.X.; Li, J.X.; Fu, S.L.; Qiu, J.P. Four New Earthworm Species Belonging to *Amynthas* Kinberg and *Metaphire* Sims et Easton (Megascolecidae: Oligochaeta) from Guangdong, China. *Ann. Zool.* **2006**, *56*, 249–254.
52. Bantaowong, U.; Chanabun, R.; James, S.W.; Panha, S. Seven New Species of the Earthworm Genus *Metaphire* Sims & Easton, 1972 from Thailand (Clitellata: Megascolecidae). *Zootaxa* **2016**, *4117*, 63. [[PubMed](#)]
53. Quan, H.W. A New Species of Earthworm from Hainan Island. *Acta Zootaxonom. Sin.* **1985**, *1*, 18–20. (In Chinese)